JACS
JOURNAL OF THE AMERICAN CHEMICAL SOCIETY

ARTICLE

pubs.acs.org/JACS

Evidence for a Thermodynamically Distinct Mg^{2+} Ion Associated with Formation of an RNA Tertiary Structure

Desirae Leipply[†] and David E. Draper[*,†,‡]

[†]Departments of Biophysics and [‡]Chemistry Johns Hopkins University Baltimore, Maryland 21218, United States

Supporting Information

ABSTRACT: A folding strategy adopted by some RNAs is to chelate cations in pockets or cavities, where the ions neutralize charge from solvent-inaccessible phosphate. Although such buried Mg^{2+}—RNA chelates could be responsible for a significant fraction of the Mg^{2+}-dependent stabilization free energy of some RNA tertiary structures, direct measurements have not been feasible because of the difficulty of finding conditions under which the free energy of Mg^{2+} chelation is uncoupled from RNA folding and from unfavorable interactions with Mg^{2+} ions in other environments. In a 58mer rRNA fragment, we have used a high-affinity thermophilic ribosomal protein to trap the RNA in a structure nearly identical to native; Mg^{2+}- and protein-stabilized structures differ in the solvent exposure of a single nucleotide located at the chelation site. Under these conditions, titration of a high affinity chelation site takes place in a micromolar range of Mg^{2+} concentration, and is partially resolved from the accumulation of Mg^{2+} in the ion atmosphere. From these experiments, we estimate the total and site-specific Mg^{2+}—RNA interaction free energies over the range of accessed Mg^{2+} concentrations. At 0.1 mM Mg^{2+} and 60 mM K^+, specific site binding contributes ~−3 kcal/mol of the total Mg^{2+} interaction free energy of ~−13 kcal/mol from all sources; at higher Mg^{2+} concentrations the site-binding contribution becomes a smaller proportion of the total (−4.5 vs −33 kcal/mol). Under approximately physiological ionic conditions, the specific binding site will be saturated but will provide only a fraction of the total free energy of Mg^{2+}—RNA interactions.

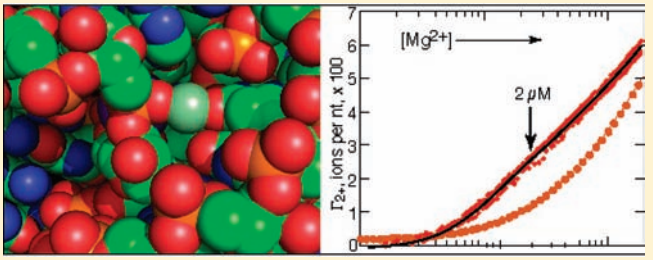

INTRODUCTION

Formation of an RNA tertiary structure brings negatively charged phosphate groups together into a compact structure that is stabilized, in part, by the accumulation of positively charged ions in and around the RNA. The role of Mg^{2+} has been of particular interest because of its ability to stabilize RNA tertiary structures by large free energies, even in the presence of more than a 100-fold excess of monovalent cations.[1−3] Two extremes have been distinguished in the ways a Mg^{2+} ion may interact with an RNA.[4] Diffuse ions remain fully hydrated and mobile at some distance from the RNA surface, interact solely with the RNA electrostatic potential, and may be responsible for most of the Mg^{2+}-dependent stabilization of many RNA tertiary structures.[5] At the other extreme, a chelated ion makes two or more direct contacts with the RNA and becomes substantially dehydrated.[6] Chelated Mg^{2+} ions were first observed in the crystal structure of the P4-P6 domain of the tetrahymena group I intron,[7] and subsequently in a small number of other RNAs, including a rRNA fragment[8] and a Mg^{2+} sensor RNA.[9] An unusual feature of chelation sites is their inclusion of backbone phosphate groups that are buried within the RNA structure and are largely inaccessible to solvent water.

RNAs with Mg^{2+} chelation sites appear much more dependent on Mg^{2+} for formation of the complete tertiary structure[10,11] than other RNAs.[12,13] Though theoretical calculations have suggested that the free energy of placing a Mg^{2+} ion in an RNA chelation site could be large,[6,14] there are no experimental measurements for comparison. Of particular interest is the magnitude of the free energy derived from binding a single ion at the chelation site compared to the total free energy available from all Mg^{2+} interactions with an RNA: in RNAs with chelation sites, do the site-bound ions dominate the Mg^{2+}-dependent energetics of folding (which would be a convenient simplification), or are other modes of Mg^{2+} interaction also important? In this work, we present experiments that attempt to answer this question for a specific RNA.

The system studied here is a small fragment of the large subunit rRNA (here called 58mer RNA, Figure 1). Previous work inferred that its intrinsic free energy for folding in the absence of Mg^{2+} is very unfavorable, roughly estimated to be as much as +19 kcal/mol (in 60 mM K^+), and predicted a commensurately large favorable interaction of the native RNA with Mg^{2+}.[15] Calculations based on the nonlinear Poisson−Boltzmann (NLPB) equation suggested that the free energy available from diffuse Mg^{2+} ions could not account for the stability of the RNA, but that a single Mg^{2+} ion, observed in the crystal structure as chelated between a phosphate nonbridging oxygen and a uracil carbonyl (Figure 1B), could provide substantial additional stabilization

Received: March 7, 2011
Published: July 21, 2011

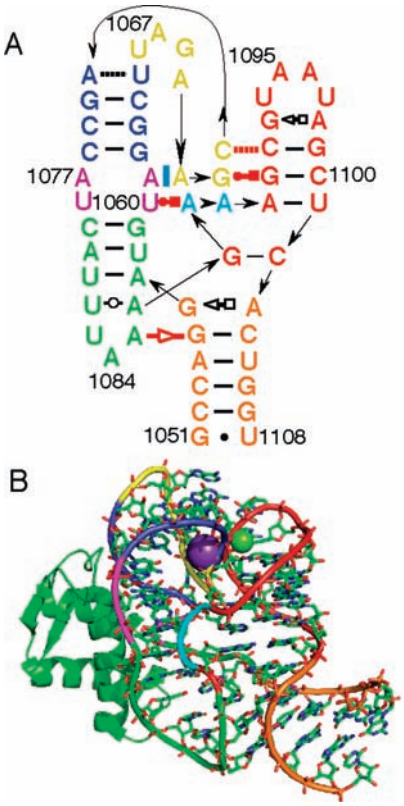

Figure 1. Depictions of the secondary and tertiary structures of the 58mer rRNA fragment with its protein binding partner. (A) Secondary structure schematic of the RNA. Arrows denote 5′−3′ backbone connectivity; secondary and tertiary base hydrogen bondings are indicated by black and red horizontal symbols, respectively, according to a standard set of symbols.[47] A cyan bar indicates extrahelical base stacking. (B) Crystal structure of 58mer RNA complexed with the C-terminal domain of ribosomal protein L11 (shown as a green ribbon). Color coding of the RNA backbone corresponds to that in panel A. Crystallographically observed ions calculated to have favorable free energies of site binding are shown as spheres: green, Mg^{2+};[6] violet, K^+.[18]

of the tertiary structure.[6,16] In principle, experimental corroboration for this calculation could come from titration of the site with Mg^{2+}, but there are two challenges in measuring Mg^{2+} site binding in this (and other) RNAs. The first is to devise a method to overcome the extreme instability of the RNA tertiary structure in the absence of Mg^{2+}. We find that a hyperthermophile homologue of the protein normally associated with the 58mer RNA domain in the intact ribosome, L11, binds the native structure tightly enough to force the RNA to fold at moderate concentrations of monovalent salt. The second potential problem is in distinguishing the titration of a single specific site from the background of interactions taking place between Mg^{2+} ions and the rest of the native RNA. An analysis of the circumstances under which this distinction may be reliably made is presented in the Background section. We present evidence that the crystallographically observed chelation site binds Mg^{2+} with an apparent intrinsic affinity of >0.5 μM^{-1} (60 mM K^+), but that the free energy derived from this site accounts for a diminishing fraction of the total Mg^{2+}−RNA interaction free energy as the Mg^{2+} concentration approaches the physiological range (less than 25% at ≥0.1 mM Mg^{2+}, 60 mM K^+).

EXPERIMENTAL METHODS

Materials. All solutions were prepared using pure water at 18.3 MΩ resistivity. High-purity (>99%) chloride salts of group I ions, KOH, and EPPS and MOPS buffers were purchased from Fluka. Buffers were adjusted to the desired pH with KOH, and KCl was added to bring the total monovalent cation concentration to 60 mM in all experiments. For experiments with other group I ions, the appropriate alkali metal hydroxide and chloride salts were used. All buffer solutions also contained 2 μM EDTA (to scavenge heavy metals without appreciably binding Mg^{2+} ion) and $MgCl_2$ as indicated. The buffer concentrations and pHs used in isothermal titrations with Mg^{2+} were the following: 20 mM EPPS, pH 8.0 (K-EPPS); or 20 mM MOPS, pH 6.8 (K-MOPS). Ten millimolar MOPS, pH 7.0, was used for melting experiments. 8-Hydroxy-5-quinolinic acid (HQS) was purchased from Sigma and recrystallized before use as described.[17] $MgCl_2$ in hexahydrate form was purchased from Sigma, and prepared $MgCl_2$ solutions were standardized by stoichiometric titration of EDTA as described.[17]

The 58mer RNA used in the experiments was obtained by *in vitro* transcriptions with T7 phage RNA polymerase from a plasmid DNA template.[18] Run-off transcriptions were purified on denaturing 16% polyacrylamide gels followed by electroelution of RNA-containing gel pieces in an Elutrap (Whatman). The sample was then concentrated and extensively exchanged into the relevant buffer using Millipore MW3 Centricon filter units (Amicon). Prior to titration experiments, RNA samples were renatured in the appropriate buffer by heating to 65 °C for 5 min, followed by incubation at room temperature for 15 min.

Expression and purification of the C-terminal 76 amino acids of *Bacillus stearothermophilus* L11 (Bst-L11c) was carried out as described.[19] The homologous 76 amino acid domain from the *Thermus thermophilus* homologue of L11 (Tth-L11c) was cloned by K. Bianchi in this laboratory from the intact gene[20] and overexpressed and purified in the same manner as Bst-L11c. Protein samples were thoroughly exchanged into the appropriate K-MOPS or K-EPPS buffers before use in experiments.

A crystal structure of the Bst-L11c complex with the 58mer RNA is available (1hc8).[21] The Tth-L11c domain has 58% sequence identity with Bst-L11c.[22] The six lysine or arginine residues of Bst-L11c that hydrogen bond to RNA phosphates in the crystal structure are conserved in Tth-L11c; in addition, the Tth protein has two sequence differences (S21 → K and E26 → K) that potentially place lysine in proximity to other phosphates.

HQS Titrations. An experimental method for measuring Γ_{2+} curves has been described in detail.[15] Briefly, automated Mg^{2+} titrations of the fluorescent indicator dye HQS (present at 10 μM) were performed in an Aviv ATF-105 fluorimeter equipped with two Hamilton titrators dispensing Mg^{2+} titrant. Experiments were carried out in K-EPPS buffer; the relatively high pH and low HQS concentration were chosen in order to access the micromolar C_{2+} range. Samples contained RNA at concentrations between 1 to 3 mg/mL (20−40 μM); no concentration dependence was observed in the experiments. The titrated samples were stirred continuously over the course of the titration and kept at 20 °C.

UV Melting Profiles. Melting profiles for the RNA in the presence of each L11 homologue were collected in a Cary 400 spectrometer. The temperature schedule for the melts included a renaturation phase (heat at 10 °C per minute to 65 °C, hold 5 min, cool to 5 at 0.66 °C per minute) and a melting phase (heat at 0.66 °C per minute to 95 °C). Up to three wavelengths were monitored, 260, 280, and 295 nm, although the large difference in extinction between 260 and 295 nm made it difficult to obtain optimum data for both of these wavelengths on the same sample. No hysteresis was observed between the cooling and heating curves.

Hydroxyl Radical Footprinting. RNA for footprinting experiments was dephosphorylated for 5′ labeling by reaction with calf

intestinal phosphatase at 37 °C for one hour, followed by phenol–chloroform extraction and ethanol precipitation to remove the enzyme and recover the RNA. Eighty picomoles of RNA was then end-labeled in 20 μL reactions with 10 μL of γ^{31}P ATP (6000 Ci/mmol, from Perkin-Elmer) and 10 units of polynucleotide kinase in the appropriate kinase buffer (New England Biolabs). Samples were gel-purified postlabeling on 16% denaturing acrylamide gels, and RNA was recovered by freeze–thaw and ethanol precipitation.

Each footprinting reaction contained 10^6 cpm of RNA in K-MOPS buffer and the desired amount of Mg^{2+} or L11c protein. On ice, H_2O_2 was added to 0.03%, and the FeEDTA complex to 1 mM ferrous ammonium sulfate and 2 mM EDTA, after degassing the solution. Reactions were quenched after 1 min with thiourea. RNA was recovered by ethanol precipitation and resuspended in 10 μL of formamide loading buffer. Five microliters of each sample, along with unreacted, alkaline hydrolysis, and T_1 RNase digest samples, were loaded on a 12% gel and run for 3 h at 70 W. The gel was then transferred to Whatman filter paper, dried, and exposed to a phosphorimager screen for 18 h. Images were analyzed and quantitated with Imagequant and SAFA.[23] Five residues (C1064, A1067, C1075, U1083, G1091, and G1099) were chosen as standards for normalization of the band intensities.

BACKGROUND

In a titration of an RNA with Mg^{2+}, it can be difficult to extract an equilibrium constant for ion binding at a specific site. The accumulation of ions simultaneously taking place in many environments in and near the RNA tends to obscure any site-specific binding of Mg^{2+};[24] in addition, the strongly repulsive interactions between a site-bound ion and other ions[6] means that the site occupancy should not follow a simple binding isotherm. In this section we elucidate conditions under which a titration curve becomes biphasic and the free energy of Mg^{2+} binding at a single site can be quantified independently of all other Mg^{2+}–RNA interactions.

The measurements made here are reported in terms of Γ_{2+}, a parameter that is conveniently defined by an equilibrium dialysis experiment. Suppose an RNA is on the "inside" of a dialysis membrane, and Mg^{2+} (among other ions) is free to pass across the membrane. At equilibrium,

$$\Gamma_{2+} \approx \frac{C_{2+}^{in} - C_{2+}^{out}}{C_{RNA}} \quad (1)$$

C_{2+}^{in} and C_{2+}^{out} are the total Mg^{2+} concentrations inside and outside of the dialysis membrane, respectively, and C_{RNA} is the total RNA concentration. In the most general terms, Γ_{2+} is the number of "excess" Mg^{2+} ions present in neutralization of the RNA charge, and its dependence on the Mg^{2+} concentration contains information about the total interaction free energy between the RNA and all Mg^{2+} ions, regardless of their environment.[25] (The remainder of the RNA charge is neutralized by an excess of monovalent ions, Γ_+ and an exclusion of anions, Γ_-.)

In this work, we reserve the terms "binding" and "binding free energy" to refer to the stoichiometric interaction of a Mg^{2+} ion with a specific chelation site, and use the generic terms "interaction" or "interaction free energy" when no specific model of the way the ions are localized is being proposed. "Binding" and "interaction" free energies are also derived by distinct thermodynamic formalisms, as detailed in Supporting Information (SI) and formalized in a thermodynamic cycle (Figure 2A). The cycle distinguishes binding of a Mg^{2+} at a single chelation site from all other Mg^{2+}–RNA interactions that might be taking place (here collectively referred to as the ion atmosphere, but potentially including ions in all possible environments). The vertical arrows describe site-binding in the presence or absence of the ion atmosphere. If only a single ion–RNA complex can be formed, the occupancy of the site in the absence of any other Mg^{2+}–RNA interactions (left vertical arrow) is given by the standard

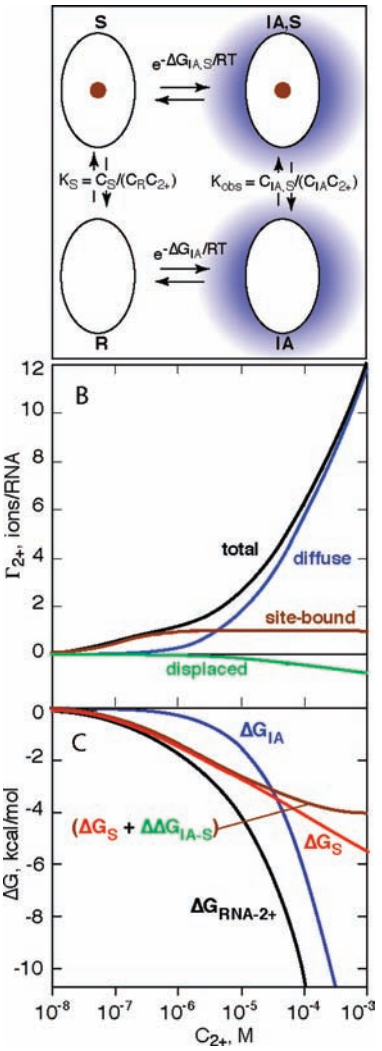

Figure 2. Mg^{2+}–RNA interactions for the 58mer RNA. (A) Thermodynamic cycle that separates site binding (vertical arrows) from accumulation of the Mg^{2+} ion atmosphere (horizontal arrows). R is RNA in the absence of interacting Mg^{2+}; S is RNA with a site-bound ion, and IA is RNA with the assembled Mg^{2+} ion atmosphere. (B) Calculations of the excess Mg^{2+} ions (Γ_{2+}) accumulated by the 58mer RNA according to the model in panel A. The intrinsic site-binding constant K_S was set to 10^7 M^{-1}, and the NLPB equation was used to find Γ_{2+} for the R and S forms. Γ_{2+} is shown for: brown, occupancy of the specific site (based on K_S, eq 3); blue, diffuse ions in the absence of a site-bound ion; green, diffuse ions "displaced" because of the occupancy of the specific site; black, the sum of site-bound, diffuse, and displaced ions. (C) Free energies of Mg^{2+} interactions with the 58mer RNA, obtained by integration of the Γ_{2+} curves in panel B: black, total free energy of Mg^{2+}–RNA interactions (ΔG_{RNA-2+}); blue, free energy of diffuse ions (ΔG_{IA}); brown, incremental free energy associated with Mg^{2+} site-binding ($\Delta G_S + \Delta\Delta G_{IA-S}$). The red curve is the intrinsic free energy of site-binding with $K_S = 10^7$ M^{-1} (eq 2).

Langmuir binding isotherm,

$$\Gamma_{2+} = \frac{K_S C_{2+}}{1 + K_S C_{2+}} \quad (2)$$

In this equation C_{2+} is the "free" ion concentration, identical to C_{2+}^{out}, and K_S is defined in terms of the observed concentrations of unbound and bound sites (R and S, respectively): $K_S = C_S/(C_R C_{2+})$.

The horizontal arrows describe the assembly of the set of all other ions (the ion atmosphere) in terms of a single free energy of Mg^{2+} interaction with the RNA; this ΔG is itself a function of C_{2+}. (As developed in the Supporting Information (SI), this interaction free energy is not associated with a difference in standard state free energies, but is derived from the change in Mg^{2+} activity coefficient caused by the presence of the RNA.) The free energy of adding the ion atmosphere to the RNA alone (ΔG_{IA}) is different than the free energy needed to create the ion atmosphere with the site-bound Mg^{2+}–RNA complex ($\Delta G_{IA,S}$) because of repulsion between Mg^{2+} at the site and Mg^{2+} in the ion atmosphere. Likewise, the observed equilibrium for site-binding is different if the ion atmosphere is present (K_S vs K_{obs}). Because the expression for K_{obs} must be independent of the path used to calculate it, the relationship

$$K_{obs} = K_S \exp(-\Delta\Delta G_{IA-S}/RT) \quad (3)$$

is obtained from the Figure 2A cycle, where $\Delta\Delta G_{IA-S}$ is the difference ($\Delta G_{IA,S} - \Delta G_{IA}$). A full derivation of eq 3 is in the Supporting Information.

To illustrate the potential appearance of experimental Mg^{2+} titration curves [Γ_{2+} vs $\log(C_{2+})$] for an RNA with a single ion binding site, we used the NLPB equation to calculate the excess Mg^{2+} (Γ_{2+}) accumulated by the 58mer RNA ion atmosphere when a single Mg^{2+} chelation site is either occupied or unoccupied. With the application of eq 3, the difference between these two calculations gives $\Delta\Delta G_{IA-S}$ as a function of C_{2+}. (The NLPB equation is based on a continuum solvent model in which all mobile ions are "diffuse", i.e. fully hydrated.[26] NLPB-based calculations underestimate experimental measurements of Γ_{2+} for the 58mer and another RNA by about 30%;[12,15] the calculations nevertheless serve as a useful illustration of the kind of titration behavior that can be expected.) When a sufficiently large K_S (eq 2) is chosen, the resulting dependence of Γ_{2+} on $\log(C_{2+})$ is biphasic (black curve, Figure 2B): the titration of the single site appears as an inflection at $C_{2+} \approx (K_S)^{-1}$, and accumulation of Mg^{2+} by the diffuse ion atmosphere takes place at higher C_{2+}. The blue curve labeled "diffuse" represents the excess Mg^{2+} that would accumulate if the specific site were unoccupied. As the specific site is titrated, the accumulation of diffuse Mg^{2+} is reduced by the amount shown as the green "displaced" curve in Figure 2B; this decrease in Γ_{2+} is a consequence of the unfavorable $\Delta\Delta G_{IA-S}$.

In Figure 2C, we compare several Mg^{2+}–RNA interaction free energies: the intrinsic free energy of binding Mg^{2+} to the specific site in the absence of any Mg^{2+} within the ion atmosphere, the actual site-binding free energy that includes the unfavorable $\Delta\Delta G_{IA-S}$, and the total interaction energy (ΔG_{RNA-2+}). (See SI for the equation used to derive ΔG values from Figure 2B titration curves by integration. Note that these free energies are functions of Mg^{2+} concentration, and are not standard state free energies.) The actual site-binding free energy becomes a progressively smaller fraction of ΔG_{RNA-2+} as the Mg^{2+} concentration increases. However, $\Delta\Delta G_{IA-S}$ negligibly affects the site occupancy (the brown curve in Figure 2B), because the site is nearly saturated before the ion atmosphere begins to accumulate.

If a value of K_S on the order of 10^5 M^{-1} is chosen for the NLPB calculation, there is no longer an inflection in the titration curve and it becomes impossible to distinguish between ion interaction models with and without specific binding sites (Figure S2 of SI). $\Delta\Delta G_{IA-S}$ also becomes large enough to nearly cancel ΔG_S; a specific site with affinity $<10^5$ M^{-1} is therefore of little net thermodynamic advantage to RNA stability. The important point for the experimental work that follows is that site-binding and ion atmosphere accumulation are approximately independent events when K_S is large enough that an inflection in the Γ_{2+} curve is observed; only then is it possible to estimate an intrinsic site-binding affinity (K_S). This conclusion applies whether the ion atmosphere consists solely of diffuse ions (as assumed in Figure 2) or includes ions in partially dehydrated environments.

RESULTS

RNA Tertiary Structure Formation in the Absence of Mg^{2+}. The C-terminal domain of ribosomal protein L11 sits in a distorted minor groove of the 58mer rRNA, where it binds to the unusual U1060-A1088 tertiary base pair[21] and thereby stabilizes the entire set of RNA tertiary contacts.[19] This protein domain from the moderate thermophile *B. stearothermophilus* (Bst-L11c) was previously shown to have a very high affinity for the 58mer RNA when sufficient $MgCl_2$ is present to ensure that the RNA tertiary structure is folded;[19,27] K_a measured at higher salt concentrations and extrapolated to 60 mM KCl is $\sim 14 \times 10^9$ M^{-1}. Despite this strong binding affinity, protein concentrations as high as 100 μM were unable to saturate the RNA in the absence of Mg^{2+} (data not shown).

A homologous L11 protein fragment from the hyperthermophile *T. thermophilus* (Tth-L11c) displayed only a stoichiometric titration of the 58mer RNA in the same assay used to measure Bst-L11c RNA affinity;[27] the Tth-L11c binding affinity must be a minimum of $\sim 10^{12}$ M^{-1} (60 mM K^+) (K. Bianchi and D.E.D., unpublished observations). This protein is able to trap the 58mer RNA tertiary structure in the absence of Mg^{2+}, as shown by melting experiments. Unfolding of the 58mer rRNA tertiary structure is uniquely associated with an unusual hypochromic change at 295 nm and the absence of any change in extinction at 280 nm.[15,28] The 295 nm signal is featureless when the RNA is melted in the absence of Mg^{2+} or protein (Figure 3A), but a ~ 10 μM excess of Tth-L11c in the absence of Mg^{2+} induces the distinctive 295 nm transition characteristic of tertiary unfolding with a T_m of ~ 38 °C (Figure 3B).

Tertiary Structure of the Tth-L11c-Bound RNA in the Absence of Mg^{2+}. In the crystal structure of the Bst-L11c–58mer RNA complex, the hairpin loop nucleotides 1069–1072 are clamped between two helices (Figure 1).[18] The hairpin backbone is wrapped around a K^+ ion that directly contacts six bridging or nonbridging phosphate oxygens (Figure 4A). The chelated K^+ and its shell of phosphate oxygens are completely buried within the solvent-accessible surface of the RNA. Presumably as a consequence of this bound ion, the 58mer RNA is most stable in the presence of K^+ and destabilized by as much as 2.7 kcal/mol when larger or smaller group I ions are present.[29] A1073 contributes one nonbridging phosphate oxygen to the K^+ and one to the chelated Mg^{2+} ion (Figure 4A).[18] We reasoned

that in the absence of Mg^{2+} to occupy the A1073 chelation site, one or more of the buried phosphates might assume alternative positions that could affect the selectivity of the RNA for K^+. This proved to be the case (Figure 5B): in melting experiments in the presence of Tth-L11c, the K^+ specificity was retained when low concentrations of Mg^{2+} were present, but completely lost in the absence of Mg^{2+}.

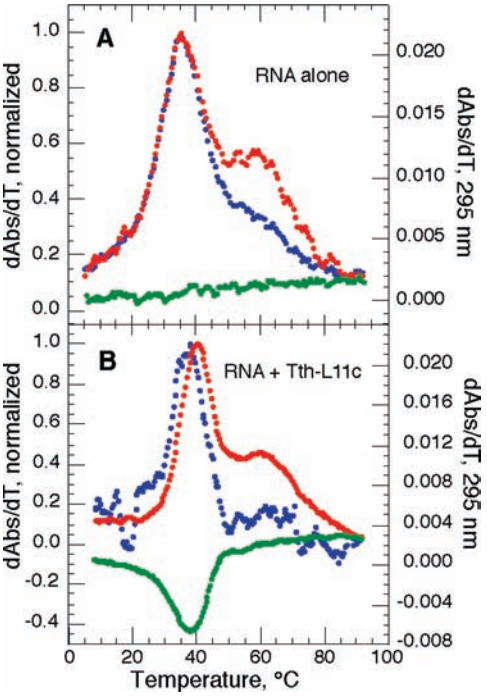

Figure 3. 58mer RNA tertiary structure is stable in the presence of Tth-L11c protein and absence of Mg^{2+}. Data were collected at three wavelengths: 260 nm (blue), 280 nm (red), and 295 nm (green) in K-MOPS buffer (60 mM K^+). In both panels, 260 and 280 nm data have been normalized (left axis) to show the slight T_m offset in the presence of protein; 295 nm data are left as the derivative of absorbance (right axis). (A) Melting profile of 58mer RNA alone (RNA at 3 μM). (B) RNA melting profile collected using 8 μM 58mer RNA and 17 μM Tth-L11c.

To assess the structural effect of Mg^{2+} omission further, we probed the RNA with hydroxyl radical. This reagent cleaves the RNA backbone via an initial reaction with the ribose sugar; the extent of reaction tends to be strongly attenuated in regions of RNA tertiary structure.[30] 58mer RNA nucleotide reactivities in the presence and absence of Mg^{2+} showed the expected protection of residues associated with formation of tertiary contacts in several regions of the RNA (Figure 4C). Especially noteworthy are the protections that were observed in the vicinity of the chelated ion sites, G1068 - A1073. In the presence of Tth-L11c (and absence of Mg^{2+}), the pattern of nucleotide reactivity for the most part either coincided with that of the Mg^{2+} - folded RNA, or showed further protections in regions where the protein contacts the RNA backbone (U1058−C1064 and C1076−U1081). These data support the inference from melting experiments (Figure 3) that Tth-L11c binds the RNA and stabilizes its overall tertiary structure in the complete absence of Mg^{2+}.

At three nucleotides, hydroxyl radical was more reactive in the Tth-L11c−RNA complex than observed in the presence of Mg^{2+} (green vertical lines, Figure 4C). At two of these nucleotides (A1077 and A1084), the same reactivity was observed in the presence of protein, whether or not Mg^{2+} was also included (SI Figure S3); perhaps protein directs hydroxyl radical to these positions. The third position, A1073, was protected by Mg^{2+} whether or not Tth-L11c was present, and unaffected by Tth-L11c alone. A1073 contributes nonbridging oxygens to both the K^+ and Mg^{2+} chelation sites (Figure 4A); its reactivity is consistent with a highly localized structural difference between the Mg^{2+}-and protein-stabilized structures, in which the absence of Mg^{2+} has allowed the two chelation pockets to open to the degree that K^+ selectivity is lost and A1073 is more exposed to solvent.

The K^+ chelation site contains three other anionic phosphate oxygens besides the one contributed by A1073 (both oxygens of C1072 and one from A1070). The resulting electrostatic potential at the K^+ chelation site is extraordinarily large, yielding an estimate for the free energy of K^+ chelation at this site as −30 kcal/mol (100 mM K^+, 1 mM Mg^{2+}).[18] Presumably the distortion of A1073 simply renders this electronegative pocket unselective toward group I ions, but does not eliminate the bound ion.

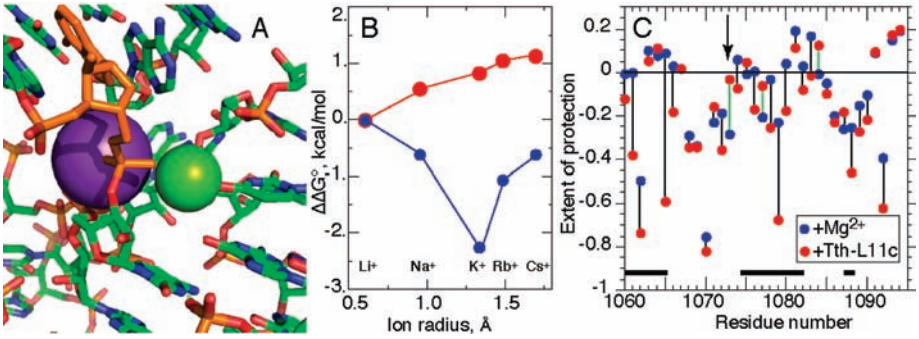

Figure 4. Evidence for incomplete folding of 58mer RNA chelation sites by Tth-L11c. (A) Chelated K^+ and Mg^{2+} (PDB 1hc8); A1073 is in orange. (B) Monovalent ion dependence of tertiary structure stability in Mg^{2+} - stabilized (blue) or Tth-L11c-stabilized (red) RNA. The relative stability of the tertiary structure, $\Delta\Delta G°$, was obtained from melting curves collected in M-MOPS buffer (where M is Li^+, Na^+, K^+, Rb^+, or Cs^+) with or without 0.5 mM $MgCl_2$ in the presence of 17 μM Tth-L11c (8 μM RNA). (C) Protection of residues from hydroxyl radical under different conditions. Protection is expressed as the difference between normalized reactivity in buffer containing 5 mM Mg^{2+} (blue) or 10 μM Tth-L11c (red) minus reactivity in control buffer containing K-MOPS buffer only; negative numbers indicate protection relative to the control. Black lines are drawn at nucleotides for which the protein confers additional protection over that observed with Mg^{2+}; green lines are residues with a greater degree of protection when protein is present. The arrow points to A1073, the residue highlighted in panel A. Relative reactivities of residues 1065−1092 were reproduced to an average of ±0.03 in independent experiments.

dx.doi.org/10.1021/ja2020923 |J. Am. Chem. Soc. 2011, 133, 13397–13405

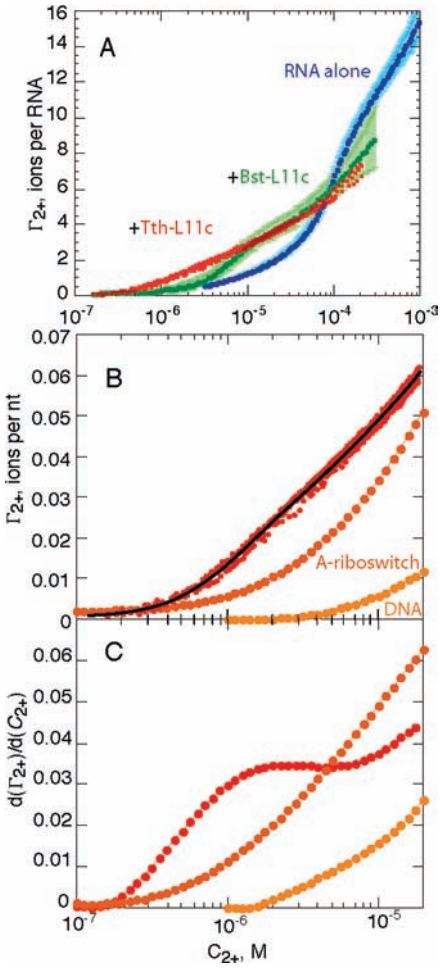

Figure 5. Γ_{2+} curves for 58mer RNA with and without L11c present (K-MOPS or K-EPPS buffer, 60 mM K^+). (A) Blue, RNA alone (data taken from 25), green, 20 μM RNA in the presence of 25 μM Bst-L11c, and red, 20 or 40 μM RNA in the presence of 10 μM excess (30 or 40 μM) Tth-L11c. Points on the RNA alone and RNA + Bst-L11c curves are the averages of three independent experiments, with error bars shown in lighter color. Individual data points from three independent titrations are shown for the RNA plus Tth-L11c curve. The *x*-axis, C_{2+}, is the bulk Mg^{2+} ion concentration, i.e. the concentration that would be measured as C_{2+}^{out} in a dialysis experiment (eq 1). (B) Red points, data for RNA plus Tth-L11c from panel A plotted with a polynomial fit to all the data points. Brown, a best-fit polynomial to Γ_{2+} data collected with the adenine riboswitch in its native conformation bound to 2,6 diaminopurine in K-MOPS buffer with 50 mM K^+.[13] Yellow, a best-fit polynomial to Γ_{2+} data collected with helical DNA in K-MOPS buffer with 60 mM K^+.[15,48] (C) First derivatives of the polynomial fits shown in panel B, with the same color coding.

Measurement of Excess Mg^{2+} (Γ_{2+}) by HQS Fluorescence Titrations. The excess Mg^{2+} associated with the 58mer RNA, Γ_{2+}, was determined by titrations with $MgCl_2$ monitored by the chelator dye HQS (Figure 5). For the 58mer RNA alone, an inflection in the Γ_{2+} curve was observed at 100 μM Mg^{2+} (60 mM K^+) (Figure 5A); this ion uptake corresponds to the midpoint of the Mg^{2+}-induced folding of the tertiary structure as detected by changes in UV absorbance at 260 and 295 nm.[15] The Γ_{2+} curve measured with an excess of Bst-L11c protein showed a similar inflection, only shifted to ~6 μM Mg^{2+} (Figure 5A). This shift is expected for a titration in which the RNA is initially in the unfolded form but can take advantage of the free energy of protein binding to adopt the native fold at lower Mg^{2+} concentrations. Because the basic Bst-L11c protein displaces some of the ion atmosphere around the RNA and neutralizes some of the RNA charge (six phosphates are directly contacted by protein basic residues[8]), Γ_{2+} for the Bst-L11c complex should not reach the same values as found for the free RNA in its native structure. Thus, the Bst-L11c−RNA complex has $\Gamma_{2+} \approx 6.2$ Mg^{2+}/RNA at 100 μM Mg^{2+}, while Γ_{2+} for the native RNA structure is estimated as 8.4 under the same conditions.[25]

If the 58mer RNA bound to Tth-L11c is folded in the absence of Mg^{2+}, the corresponding Γ_{2+} curve for the complex should lack any sharp uptake of Mg^{2+} associated with a folding transition. The Tth-L11c protein did increase the values of Γ_{2+} at Mg^{2+} concentrations below ~10 μM, and seemed to eliminate the folding transition seen in the presence of Bst-L11c (Figure 5A). The Γ_{2+} curve for the Tth-L11c−RNA complex is compared with Γ_{2+} data collected with other nucleic acids in Figure 5B. Duplex DNA at the same monovalent salt concentration (60 mM K^+) interacts much more weakly with Mg^{2+}, which is perhaps to be expected: DNA has a high charge density which easily accumulates Mg^{2+} in preference to K^+,[26] but the close juxtaposition of phosphates in some RNA tertiary structures may develop much more intense electrostatic potentials.[24] A more telling comparison is with the aptamer of the adenine riboswitch (71 nt), which creates a high charge density pocket around a bound purine ligand and might be expected to interact strongly with Mg^{2+}.[31,32] The native RNA structure is formed in the complete absence of Mg^{2+} if a high concentration of ligand is added; therefore, in the titration shown (Figure 5B), the RNA was in its fully folded conformation over the entire range of C_{2+}.[13] The riboswitch Γ_{2+} curve is strikingly different from the Tth-L11c−RNA curve. Even though the 58mer RNA is being held at a slightly higher salt concentration (60 mM K^+, vs 50 mM for the riboswitch) in the presence of a basic protein, both factors that should reduce Γ_{2+}, it interacts much more strongly with Mg^{2+} at C_{2+} concentrations up to 10 μM.

An unusual feature of the Tth-L11c−RNA titration curve is the appearance of an inflection at ~2.0 μM C_{2+}, which is apparent from the first derivative of the Γ_{2+} curve (Figure 5C). The first derivative of the DNA and riboswitch curves are strongly concave upward over the same region (Figure 5C). We interpret this inflection as evidence of Mg^{2+} binding to a specific RNA site with $K_S \approx 0.5$ μM^{-1} (see Discussion of Figure 2 in Background), and suppose that the distinctive sigmoid shape of the site titration has been nearly overwhelmed by contributions from Mg^{2+} accumulation in the ion atmosphere at higher C_{2+}.[33] To ask what site-binding stoichiometry could be accommodated, we subtracted Γ_{2+} for a single site binding isotherm ($K_S \approx 0.5$ μM^{-1}) from the 58mer RNA Γ_{2+} curve (Figure S3 of SI); the difference approximates the expected contribution of the ion atmosphere. (NLPB calculations indicate that, up to a Mg^{2+} concentration of 10 μM, the nonadditivity of chelated and diffuse ion contributions to Γ_{2+} has only a small effect on the subtracted curve, lowering it by a maximum of about 0.16 ions/RNA.) This residual curve lies at higher Γ_{2+} values than calculated for diffuse ions using the NLPB equation, but if a stoichiometry of two ions is assumed, the subtracted curve lies well below the calculated diffuse ion Γ_{2+} values. As NLPB calculations tend to underestimate Γ_{2+} for this RNA at higher C_{2+},[15] we take a single ion binding site as the most likely explanation for the presence of the inflection in the titration curve (see Discussion).

DISCUSSION

Titration of a High-Affinity Mg^{2+} Binding Site. By crystallography, chelated Mg^{2+} ions have been seen partially or completely buried within some RNA structures, and the occupancy of such sites has been presumed crucial for achieving the native fold.[34,35] The tight coupling between RNA folding and Mg^{2+} chelation, and the strong interactions between ions in different environments has made it difficult to study Mg^{2+} chelation independently of all the other RNA−ion interactions taking place in an RNA.[10,36,37] In this work we have asked whether Mg^{2+} binding to a crystallographically observed chelation site can be distinguished in solution titrations and how the corresponding binding free energy compares in magnitude to the total Mg^{2+}−RNA interaction free energy, ΔG_{RNA-2+}.

Our simulations of titration data (Figure 2 and Figure S3 in the SI) show that occupancy of a chelation site and accumulation of Mg^{2+} in the ion atmosphere become independent if the site binds Mg^{2+} tightly enough; it is then possible to estimate an intrinsic site-binding free energy (ΔG_S). We interpret the Γ_{2+} titration curve of the Tth-L11c−RNA complex in these terms (Figure 5B); that is, the unusually strong interaction of the RNA with micromolar concentrations of Mg^{2+} and the appearance of an inflection at ~2 μM Mg^{2+} are consistent with ion binding at a high affinity site, though the site does not become fully saturated before excess Mg^{2+} ions start to accumulate because of interactions with other parts of the RNA. (This interpretation does not rule out the possibility that there are other weaker chelation sites.) In the discussion that follows, we identify the high affinity binding site with the Mg^{2+} chelated at A1073 in the crystal structure (Figure 1B). Calculations carried out on all 11 crystallographically observed Mg^{2+} found that, by a large margin, only the A1073 site had a strong enough electrostatic potential to overcome the large Mg^{2+} dehydration energy and other penalties associated with chelation.[6]

How important is the high-affinity Mg^{2+} binding site to the overall Mg^{2+}-dependent energetics of this RNA? The answer to this question depends on the particular Mg^{2+} concentration under consideration (compare the varying ratio of the site-binding energy, $\Delta G_s + \Delta\Delta G_{IA-S}$, to ΔG_{RNA-2+} in Figure 2C). We start with 0.1 mM Mg^{2+} (in a background of 60 mM K^+) as a convenient reference concentration for making comparisons. Uncertainties in our titration data become larger at higher concentrations (Figure 5A), and at the 60 mM K^+ concentrations present in our titrations, 0.1 mM Mg^{2+} is also an approximation of *in vivo* conditions. The activity of cations in *E. coli* is roughly equivalent to a solution of 0.15 M KCl and 0.5 − 1 mM $MgCl_2$ (see references cited in[38]). As 0.15 M K^+ shifts the 58mer RNA Γ_{2+} curve to about 5-fold higher Mg^{2+} concentrations than obtained in 60 mM K^+,[15] the RNA negative charge is neutralized by 0.1 mM Mg^{2+} in our experiments to an approximately similar extent as it would be *in vivo*.

To evaluate the net Mg^{2+} site-binding free energy, three free energies must be assessed:

First, there is an intrinsic free energy of Mg^{2+} binding at the chelation site, ΔG_S. If the site is half-saturated at 2 μM, appropriate integration of the standard binding isotherm (eq 2) gives $\Delta G_S = -2.2$ kcal/mol at 0.1 mM Mg^{2+}.[33]

Second, unfavorable interactions of the site-bound ion with other Mg^{2+} ions in and near the RNA reduce the free energy increment associated with site-binding. NLPB calculations for diffuse ions suggest that this factor ($\Delta\Delta G_{IA-S}$) is ~+0.5 kcal/mol when Mg^{2+} is at 0.1 mM (Figure 2B).

Third, the Mg^{2+} chelation site is not identical in conformation to the native structure, as indicated by the lack of K^+ selectivity and exposure of A1073 to solvent (Figure 4). Mg^{2+} binding at this site is therefore coupled to a local conformational rearrangement of the RNA. On the basis of simple estimates of the Coulombic free energy of moving the A1073 phosphate a few ångstroms away from the three closest phosphates (4−6 Å distant), and presuming that electrostatic forces will dominate the free energy of the conformational change, we estimate that the conformational change associated with ion chelation could cost ~1 kcal/mol of binding free energy. If nucleotides in addition to A1073 have moved, the energetic cost of the rearrangement could be larger.

Summing the measured ΔG_S, the calculated value for $\Delta\Delta G_{IA-S}$, and the estimated correction for the A1073 conformational change, the presence of the chelated ion stabilizes the RNA by a free energy of ~−2.7 kcal/mol, compared to a hypothetical situation in which only the ion atmosphere stabilizes the native structure (at our reference of 0.1 mM Mg^{2+} and 60 mM K^+).

The total free energy of Mg^{2+}−RNA interaction is obtained by integration of the Γ_{2+} titration curve (see SI). Using Γ_{2+} for the Tth-L11c−RNA complex (Figure 5B), we find ΔG_{RNA-2+} = −8.3 kcal/mol when the Mg^{2+} concentration is 0.1 mM. As already noted, the bound protein neutralizes some of the RNA charge and reduces Γ_{2+} from that of the native RNA by about 30% at 0.1 mM Mg^{2+}. Scaling the entire Γ_{2+} curve by this factor brings the Mg^{2+} interaction free energy for the native RNA itself to ~−11.8 kcal/mol. After allowing ~1 kcal/mol for the free energy of chelation site conformational rearrangement, our estimate for ΔG_{RNA-2+} comes to ~−12.8 kcal/mol (0.1 mM Mg^{2+}). The single site-bound ion is therefore a significant factor in the overall RNA folding energetics, though its binding free energy is still outweighed by about a 4-fold greater contribution from the ion atmosphere.

The relative importance of the chelation site diminishes at Mg^{2+} concentrations greater than 0.1 mM. As seen in the titration of 58mer RNA alone (Figure 5A), Γ_{2+} for the native RNA continues to increase steeply as C_{2+} approaches 1 mM; based on this curve, we estimate $\Delta G_{RNA-2+} \approx -33$ kcal/mol at 1 mM Mg^{2+}. The intrinsic Mg^{2+} site-binding free energy also increases, to −4.5 kcal/mol (1 mM Mg^{2+}). The interaction of the site-bound ion with other Mg^{2+} ($\Delta\Delta G_{IA-S}$) will become more unfavorable; NLPB-based calculations estimate $\Delta\Delta G_{IA-S} \approx$ +1.2 kcal/mol. Together with the 1 kcal/mol correction for the local conformational change at the chelation site, the site-bound ion contributes ~−4.3 kcal/mol, 13% of the total Mg^{2+}−RNA interaction free energy at 1 mM Mg^{2+}.

As a final comparison, the total free energy for 0.1 mM Mg^{2+} interacting with the unfolded RNA is ΔG_{RNA-2+} = −3.6 kcal/mol, obtained with an RNA variant unable to form the native structure in similar titrations as shown in Figure 5.[25] The net stabilization free energy available from 0.1 mM Mg^{2+} is the difference between the native and unfolded ΔG_{RNA-2+}, about −9 kcal/mol. As 0.1 mM is about the concentration of Mg^{2+} needed to bring folded and unfolded RNA to equal concentrations (the observed free energy of folding is zero), the native conformation of the RNA is therefore unstable by a very substantial ~9 kcal/mol in the absence of Mg^{2+}. (A previous estimate of this energy, 19 kcal/mol, was based on an extrapolation from RNA folding under extreme salt conditions, 1.6 M NH_4Cl, and had the potential for large errors.[25]) This instability of the 58mer RNA without Mg^{2+}

contrasts with many RNA tertiary structures that fold stably in the complete absence of Mg^{2+},[12,13,39] and underscores the dependence of this rRNA fragment on Mg^{2+}.

Thermodynamic and Structural Significance of Ion Chelation Sites in RNA. A salient feature of the chelated Mg^{2+} studied in this work is the direct interaction of anionic oxygens from a single phosphate, A1073, to both the chelated Mg^{2+} and a nearby buried K^+ ion (Figure 1). As the presence of a positive charge 5.7 Å away must reduce the Mg^{2+} binding free energy to some degree, it might be thought that isolated chelation sites would be favored in the evolution of stable RNA structures. However, a large fraction of the known Mg^{2+} chelation sites features a single phosphate directly contacting two cations. Thus, two Mg^{2+} share a common phosphate in the P4−P6 domain of the group I intron[34] and in a glycine-binding aptamer.[40] A Mg^{2+} riboswitch (M-box) RNA has an impressive array of three Mg^{2+} and three K^+ linked by several shared phosphates,[9] and the ribosome 50S subunit also has several instances of this motif (C162 contacts Mg^{2+} and K^+; A1839 and C2534 both contact pairs of Mg^{2+} ions).[41] Perhaps geometric constraints of burying ion−phosphate pairs make this shared-phosphate arrangement preferred.

In all instances where a single phosphate contributes to two ion chelation sites, the phosphate is largely sequestered within the RNA solvent-accessible surface. The energetic cost of folding RNA to form such a structure should be very high: transfer of phosphates from water to solvent-inaccessible positions within the RNA entails a substantial dehydration penalty,[18,34] and the negative electrostatic potential created at these sites is extremely high.[6,42] These dehydration and electrostatic costs are large enough in the 58mer and P4−P6 RNAs that, in the absence of Mg^{2+}, the chelating phosphates become solvent exposed under conditions that allow formation of other tertiary interactions within the RNA.[36] The unfavorable free energy of chelation site formation is of course compensated by the favorable free energy of cation binding. Alternatively, high concentrations of an osmolyte sufficiently reduce the penalty for phosphate dehydration that the 58mer RNA A1073 chelation site forms correctly in the absence of Mg^{2+}.[43]

The net stabilization free energy available to an RNA from formation of an ion−phosphate chelate is difficult to estimate, but the magnitude of the site-binding free energy (−2.7 to −4.5 kcal/mol in 0.1−1.0 mM Mg^{2+}, 60 mM K^+) compared to the large instability of the 58mer RNA in the absence of Mg^{2+} (+9 kcal/mol) suggests to us that specific ion binding only offsets the energetic penalty of forming the chelation site. (The 58mer domain of *E. coli* rRNA is in fact marginally stable and relies on the L11 protein for its overall stability *in vivo*.[44,45]) Thus, we think it unlikely that chelation sites have been selected to confer extra stability on RNAs. Instead, we suggest that chelation sites allow RNAs to explore backbone configurations that have solvent-inaccessible phosphate and would not be energetically feasible in the absence of the free energy derived from site-bound cations.

CONCLUSIONS

The very high affinity of a ribosomal protein for an rRNA fragment with a compact tertiary structure has afforded an opportunity to observe binding of a Mg^{2+} ion at a chelation site created, in part, by the burial of a phosphate (A1073) within the RNA structure. The free energy of placing an ion at this site is substantial but less than a quarter of the total free energy of all Mg^{2+} ions interacting with the native RNA at concentrations $\geq$0.1 mM (with 60 mM K^+). Although this estimate comes with caveats (neither the unfavorable interaction between the site-bound ion and other Mg^{2+} ions nor the free energy of the conformational change in A1073 can be experimentally measured, and neither is likely to be negligible), when considered with other data it has important implications for RNA folding studies. On the one hand, it appears that solvent-inaccessible phosphates are very destabilizing to an RNA, and a large free energy from ion chelation is necessary to drive the RNA into its native structure. RNA native structures may therefore differ considerably in their sensitivity to the concentrations and types of ions present, depending on the existence and specificity of ion chelation sites within the RNA. On the other hand, the free energy of binding Mg^{2+} to the chelation site is not overwhelming: the majority of the Mg^{2+}-dependent free energy must come from ions distributed among other kinds of environments. Although early studies of tRNA had supposed that the Mg^{2+}-dependent stability of these structures could be explained by ions bound at one or a few specific sites,[46] this idea now seems unlikely to be true for any RNA, except under extreme conditions.

ASSOCIATED CONTENT

Supporting Information. Derivation of the equations used to calculate the curves presented in Figure 2, and an additional figure of hydroxyl radical protection data. This material is available free of charge via the Internet at http://pubs.acs.org.

AUTHOR INFORMATION

Corresponding Author
draper@jhu.edu

ACKNOWLEDGMENT

This work was supported by National Institutes of Health Grants RO1 GM58545 (to D.E.D.) and T32 GM008403 (Program in Molecular Biophysics).

REFERENCES

(1) Lynch, D. C.; Schimmel, P. R. *Biochemistry* **1974**, *13*, 1841–1852.
(2) Römer, R.; Hach, R. *Eur. J. Biochem.* **1975**, *55*, 271–284.
(3) Stein, A.; Crothers, D. M. *Biochemistry* **1976**, *15*, 160–167.
(4) Draper, D. E.; Grilley, D.; Soto, A. M. *Annu. Rev. Biophys. Biomol. Struct.* **2005**, *34*, 221–243.
(5) Misra, V. K.; Draper, D. E. *Biopolymers* **1998**, *48*, 113–135.
(6) Misra, V. K.; Draper, D. E. *Proc. Natl. Acad. Sci. U.S.A.* **2001**, *98*, 12456–12461.
(7) Cate, J. H.; Doudna, J. A. *Structure* **1996**, *15*, 1221–1229.
(8) Conn, G. L.; Draper, D. E. *Curr. Opin. Struct. Biol.* **1998**, *8*, 278–285.
(9) Dann, C. E., 3rd; Wakeman, C. A.; Sieling, C. L.; Baker, S. C.; Irnov, I.; Winkler, W. C. *Cell* **2007**, *130*, 878–892.
(10) Bukhman, Y. V.; Draper, D. E. *J. Mol. Biol.* **1997**, *273*, 1020–1031.
(11) Takamoto, K.; He, Q.; Morris, S.; Chance, M. R.; Brenowitz, M. *Nat. Struct. Biol.* **2002**, *9*, 928–933.
(12) Soto, A. M.; Misra, V.; Draper, D. E. *Biochemistry* **2007**, *46*, 2973–2983.
(13) Leipply, D.; Draper, D. E. *Biochemistry* **2010**, *49*, 1843–1853.
(14) Petrov, A. S.; Lamm, G.; Pack, G. R. *Biopolymers* **2005**, *77*, 137–154.

(15) Grilley, D.; Misra, V.; Caliskan, G.; Draper, D. E. *Biochemistry* **2007**, *46*, 10266–10278.
(16) Misra, V. K.; Draper, D. E. *J. Mol. Biol.* **2002**, *317*, 507–521.
(17) Grilley, D.; Soto, A. M.; Draper, D. E. *Methods Enzymol.* **2009**, *455*, 71–94.
(18) Conn, G. L.; Gittis, A. G.; Lattman, E. E.; Misra, V. K.; Draper, D. E. *J. Mol. Biol.* **2002**, *318*, 963–973.
(19) Xing, Y.; Draper, D. E. *J. Mol. Biol.* **1995**, *249*, 319–331.
(20) Lee, D.; Walsh, J. D.; Yu, P.; Markus, M. A.; Choli-Papadopoulou, T.; Schwieters, C. D.; Krueger, S.; Draper, D. E.; Wang, Y. X. *J. Mol. Biol.* **2007**, *367*, 1007–1022.
(21) Conn, G. L.; Draper, D. E.; Lattman, E. E.; Gittis, A. G. *Science* **1999**, *284*, 1171–1174.
(22) Triantafillidou, D.; Simitsopoulou, M.; Franceschi, F.; Choli-Papadopoulou, T. *J. Protein Chem.* **1999**, *18*, 215–223.
(23) Das, R.; Laederach, A.; Pearlman, S. M.; Herschlag, D.; Altman, R. B. *RNA* **2005**, *11*, 344–354.
(24) Misra, V. K.; Draper, D. E. *J. Mol. Biol.* **2000**, *299*, 813–825.
(25) Grilley, D.; Soto, A. M.; Draper, D. E. *Proc. Natl. Acad. Sci. U.S.A.* **2006**, *103*, 14003–14008.
(26) Misra, V. K.; Draper, D. E. *J. Mol. Biol.* **1999**, *294*, 1135–1147.
(27) Bausch, S. L.; Poliakova, E.; Draper, D. E. *J. Biol. Chem.* **2005**, *280*, 29956–29963.
(28) Lu, C.; Smith, A. M.; Fuchs, R. T.; Ding, F.; Rajashankar, K.; Henkin, T. M.; Ke, A. *Nat. Struct. Mol. Biol.* **2008**, *15*, 1076–1083.
(29) Shiman, R.; Draper, D. E. *J. Mol. Biol.* **2000**, *302*, 79–91.
(30) Latham, J. A.; Cech, T. R. *Science* **1989**, *245*, 276–245.
(31) Serganov, A.; Yuan, Y. R.; Pikovskaya, O.; Polonskaia, A.; Malinina, L.; Phan, A. T.; Hobartner, C.; Micura, R.; Breaker, R. R.; Patel, D. J. *Chem. Biol.* **2004**, *11*, 1729–1741.
(32) Rieder, R.; Lang, K.; Graber, D.; Micura, R. *ChemBioChem* **2007**, *8*, 896–902.
(33) The main source of error in our estimation of $K_S \approx 0.5\,\mu M^{-1}$ is differentiating site-binding and ion atmosphere contributions to Γ_{2+}; the ion atmosphere should offset the midpoint of the site-binding isotherm to a lower value of Γ_{2+} than the actual inflection in the Γ_{2+} curve. The most extreme offset that can be accommodated by the data moves the titration midpoint from 2.0 μM to 1.6 μM. This shift would make the Mg^{2+} ion site-binding free energy 0.1 kcal/mol more negative at $C_{2+} \geq 0.1$ mM.
(34) Cate, J. H.; Hanna, R. L.; Doudna, J. A. *Nat. Struct. Biol.* **1997**, *4*, 553–558.
(35) Wakeman, C. A.; Ramesh, A.; Winkler, W. C. *J. Mol. Biol.* **2009**, *392*, 723–735.
(36) Das, R.; Travers, K. J.; Bai, Y.; Herschlag, D. *J. Am. Chem. Soc.* **2005**, *127*, 8272–8273.
(37) Horton, T. E.; Clardy, D. R.; DeRose, V. J. *Biochemistry* **1998**, *37*, 18094–18101.
(38) Draper, D. E. *Biophys. J.* **2008**, *95*, 5489–5495.
(39) Cole, P. E.; Yang, S. K.; Crothers, D. M. *Biochemistry* **1972**, *11*, 4358–4368.
(40) Huang, L.; Serganov, A.; Patel, D. J. *Mol. Cell* **2010**, *40*, 774–786.
(41) Klein, D. J.; Moore, P. B.; Steitz, T. A. *RNA* **2004**, *10*, 1366–1379.
(42) Chin, K.; Sharp, K. A.; Honig, B.; Pyle, A. M. *Nat. Struct. Biol.* **1999**, *6*, 1055–1061.
(43) Lambert, D.; Leipply, D.; Draper, D. E. *J. Mol. Biol.* **2010**, *404*, 138–157.
(44) Laing, L. G.; Draper, D. E. *J. Mol. Biol.* **1994**, *237*, 560–576.
(45) Maeder, C.; Conn, G. L.; Draper, D. E. *Biochemistry* **2006**, *45*, 6635–6643.
(46) Schimmel, P. R.; Redfield, A. G. *Annu. Rev. Biophys. Bioeng.* **1980**, *9*, 181–221.
(47) Leontis, N. B.; Westhof, E. *RNA* **2001**, *7*, 499–512.
(48) Grilley, D. PhD. Dissertation, Johns Hopkins University, Baltimore, 2005.